Control Optimization

Dehaeze Thomas

April 3, 2025

Contents

When controlling a MIMO system (specifically parallel manipulator such as the Stewart platform?)

Several considerations:

- Section 1: How to most effectively use/combine multiple sensors
- Section 2: How to decouple a system
- Section 3: How to design the controller

1 Multiple Sensor Control

Look at what was done in the introduction Stewart platforms: Control architecture

Explain why multiple sensors are sometimes beneficial:

- collocated sensor that guarantee stability, but is still useful to damp modes outside the bandwidth of the controller using sensor measuring the performance objective

- Review for Stewart platform =¿ Table Multi Sensor Control Several sensors:

    - force sensor, inertial, strain ...

  Several architectures:

    - Sensor fusion

    - Cascaded control

    - Two sensor control

  [1] [2]

Cascaded control / HAC-LAC Architecture was already discussed during the conceptual phase. This is a very comprehensive approach that proved to give good performances.

On the other hand of the spectrum, the two sensor approach yields to more control design freedom. But it is also more complex.

In this section, we wish to study if sensor fusion can be an option for multi-sensor control:
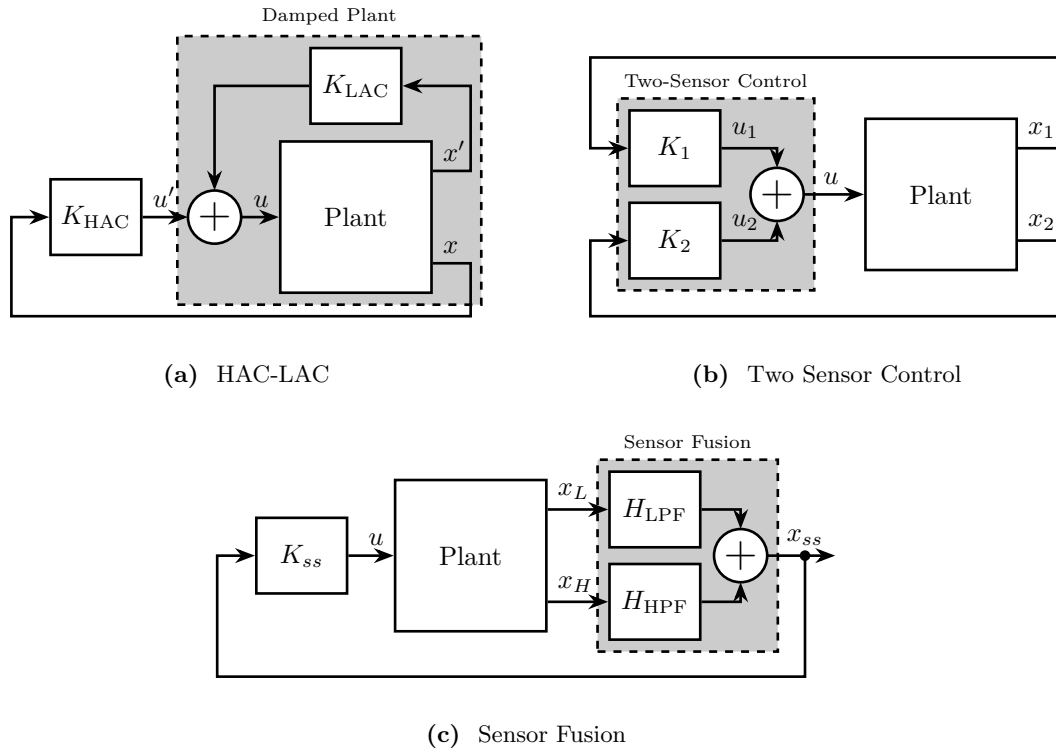
- may be used to optimize the noise characteristics

- optimize the dynamical uncertainty

While there are different ways to fuse sensors:

- complementary filters

- kalman filtering

The focus is made here on complementary filters, as they give a simple frequency analysis.

Measuring a physical quantity using sensors is always subject to several limitations. First, the accuracy of the measurement is affected by several noise sources, such as electrical noise of the conditioning

(a) HAC-LAC

(b) Two Sensor Control

(c) Sensor Fusion

Figure 1.1: Different control strategies when using multiple sensors. High Authority Control / Low Authority Control (a). Sensor Fusion (c). Two-Sensor Control (b)

electronics being used. Second, the frequency range in which the measurement is relevant is bounded by the bandwidth of the sensor. One way to overcome these limitations is to combine several sensors using a technique called "sensor fusion" [3]. Fortunately, a wide variety of sensors exists, each with different characteristics. By carefully choosing the fused sensors, a so called "super sensor" is obtained that can combines benefits of the individual sensors.

In some situations, sensor fusion is used to increase the bandwidth of the measurement [4], [5], [6]. For instance, in [4] the bandwidth of a position sensor is increased by fusing it with an accelerometer providing the high frequency motion information. For other applications, sensor fusion is used to obtain an estimate of the measured quantity with lower noise [7], [8], [9], [10]. More recently, the fusion of sensors measuring different physical quantities has been proposed to obtain interesting properties for control [2], [11]. In [11], an inertial sensor used for active vibration isolation is fused with a sensor collocated with the actuator for improving the stability margins of the feedback controller.

Practical applications of sensor fusion are numerous. It is widely used for the attitude estimation of several autonomous vehicles such as unmanned aerial vehicle [12], [13], [14] and underwater vehicles [15], [16]. Naturally, it is of great benefits for high performance positioning control as shown in [2], [4], [5], [6]. Sensor fusion was also shown to be a key technology to improve the performance of active vibration isolation systems [17]. Emblematic examples are the isolation stages of gravitational wave detectors [11], [18] such as the ones used at the LIGO [7], [8] and at the Virgo [19].

There are mainly two ways to perform sensor fusion: either using a set of complementary filters [20] or using Kalman filtering [21]. For sensor fusion applications, both methods are sharing many relationships [10], [21], [22], [23]. However, for Kalman filtering, assumptions must be made about the probabilistic character of the sensor noises [10] whereas it is not the case with complementary filters. Furthermore, the advantages of complementary filters over Kalman filtering for sensor fusion are their general applicability, their low computational cost [22], and the fact that they are intuitive as their effects can be easily interpreted in the frequency domain.

A set of filters is said to be complementary if the sum of their transfer functions is equal to one at all frequencies. In the early days of complementary filtering, analog circuits were employed to physically realize the filters [20]. Analog complementary filters are still used today [2], [24], but most of the time they are now implemented digitally as it allows for much more flexibility.

Several design methods have been developed over the years to optimize complementary filters. The easiest way to design complementary filters is to use analytical formulas. Depending on the application, the formulas used are of first order [2], [13], [25], second order [12], [14], [26] or even higher orders [4], [5], [11], [26], [27].

As the characteristics of the super sensor depends on the proper design of the complementary filters [28], several optimization techniques have been developed. Some are based on the finding of optimal parameters of analytical formulas [6], [14], [23], while other are using convex optimization tools [7], [8] such as linear matrix inequalities [15]. As shown in [9], the design of complementary filters can also be linked to the standard mixed-sensitivity control problem. Therefore, all the powerful tools developed for the classical control theory can also be used for the design of complementary filters. For instance, in [14] the two gains of a Proportional Integral (PI) controller are optimized to minimize the noise of the super sensor.

The common objective of all these complementary filters design methods is to obtain a super sensor that has desired characteristics, usually in terms of noise and dynamics. Moreover, as reported in [5], [9], phase shifts and magnitude bumps of the super sensors dynamics can be observed if either the complementary filters are poorly designed or if the sensors are not well calibrated. Hence, the robustness of the fusion is also of concern when designing the complementary filters. Although many

design methods of complementary filters have been proposed in the literature, no simple method that allows to specify the desired super sensor characteristic while ensuring good fusion robustness has been proposed.

Fortunately, both the robustness of the fusion and the super sensor characteristics can be linked to the magnitude of the complementary filters [28]. Based on that, this paper introduces a new way to design complementary filters using the $\mathcal{H}_\infty$ synthesis which allows to shape the complementary filters' magnitude in an easy and intuitive way.
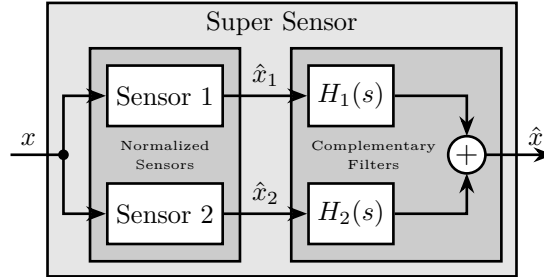
1.1 Sensor Fusion and Complementary Filters Requirements

Complementary filtering provides a framework for fusing signals from different sensors. As the effectiveness of the fusion depends on the proper design of the complementary filters, they are expected to fulfill certain requirements. These requirements are discussed in this section.

1.1.1 Sensor Fusion Architecture

A general sensor fusion architecture using complementary filters is shown in Fig. 1.2 where several sensors (here two) are measuring the same physical quantity x. The two sensors output signals $\hat{x}_1$ and $\hat{x}_2$ are estimates of x. These estimates are then filtered out by complementary filters and combined to form a new estimate $\hat{x}$.

The resulting sensor, termed as super sensor, can have larger bandwidth and better noise characteristics in comparison to the individual sensors. This means that the super sensor provides an estimate $\hat{x}$ of x which can be more accurate over a larger frequency band than the outputs of the individual sensors.

Figure 1.2: Schematic of a sensor fusion architecture using complementary filters.

The complementary property of filters $H_1(s)$ and $H_2(s)$ implies that the sum of their transfer functions is equal to one. That is, unity magnitude and zero phase at all frequencies. Therefore, a pair of complementary filter needs to satisfy the following condition:

$$H_1(s) + H_2(s) = 1 \tag{1.1}$$

It will soon become clear why the complementary property is important for the sensor fusion architecture.

1.1.2 Sensor Models and Sensor Normalization

In order to study such sensor fusion architecture, a model for the sensors is required. Such model is shown in Fig. 1.3a and consists of a linear time invariant (LTI) system $G_i(s)$ representing the sensor dynamics and an input n_i representing the sensor noise. The model input x is the measured physical quantity and its output $\tilde{x}_i$ is the "raw" output of the sensor.

Before filtering the sensor outputs $\tilde{x}_i$ by the complementary filters, the sensors are usually normalized to simplify the fusion. This normalization consists of using an estimate $\hat{G}_i(s)$ of the sensor dynamics $G_i(s)$, and filtering the sensor output by the inverse of this estimate $\hat{G}_i^{-1}(s)$ as shown in Fig. 1.3b. It is here supposed that the sensor inverse $\hat{G}_i^{-1}(s)$ is proper and stable. This way, the units of the estimates $\hat{x}_i$ are equal to the units of the physical quantity x. The sensor dynamics estimate $\hat{G}_i(s)$ can be a simple gain or a more complex transfer function.
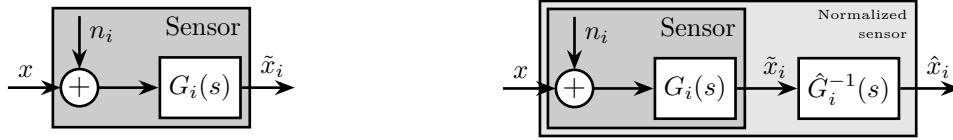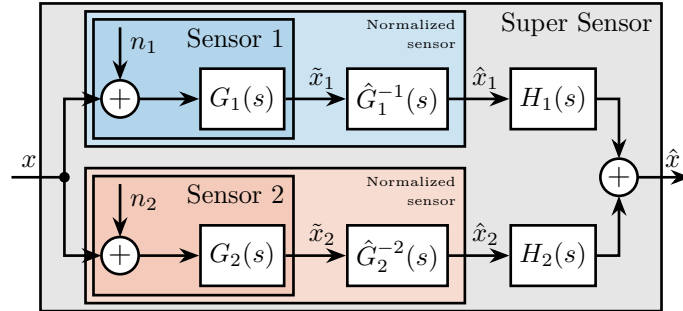

(a) Basic sensor model consisting of a noise input n_i and a linear time invariant transfer function $G_i(s)$

(b) Normalized sensors using the inverse of an estimate $\hat{G}$

Figure 1.3: Sensor models with and without normalization.

Two normalized sensors are then combined to form a super sensor as shown in Fig. 1.4. The two sensors are measuring the same physical quantity x with dynamics $G_1(s)$ and $G_2(s)$, and with *uncorrelated* noises n_1 and n_2. The signals from both normalized sensors are fed into two complementary filters $H_1(s)$ and $H_2(s)$ and then combined to yield an estimate $\hat{x}$ of x.

The super sensor output is therefore equal to:

$$\hat{x} = \left(H_1(s)\hat{G}_1^{-1}(s)G_1(s) + H_2(s)\hat{G}_2^{-1}(s)G_2(s) \right)x + H_1(s)\hat{G}_1^{-1}(s)G_1(s)n_1 + H_2(s)\hat{G}_2^{-1}(s)G_2(s)n_2 \quad (1.2)$$

Figure 1.4: Sensor fusion architecture with two normalized sensors.

1.1.3 Noise Sensor Filtering

In this section, it is supposed that all the sensors are perfectly normalized, such that:

$$\frac{\hat{x}_i}{x} = \hat{G}_i(s)G_i(s) = 1 \tag{1.3}$$

The effect of a non-perfect normalization will be discussed in the next section.

Provided (1.3) is verified, the super sensor output $\hat{x}$ is then equal to:

$$\hat{x} = x + H_1(s)n_1 + H_2(s)n_2 \tag{1.4}$$

From (1.4), the complementary filters $H_1(s)$ and $H_2(s)$ are shown to only operate on the noise of the sensors. Thus, this sensor fusion architecture permits to filter the noise of both sensors without introducing any distortion in the physical quantity to be measured. This is why the two filters must be complementary.

The estimation error δx, defined as the difference between the sensor output $\hat{x}$ and the measured quantity x, is computed for the super sensor (1.5).

$$\delta x \hat{x} - x = H_1(s)n_1 + H_2(s)n_2 \tag{1.5}$$

As shown in (1.6), the Power Spectral Density (PSD) of the estimation error $\Phi_{\delta x}$ depends both on the norm of the two complementary filters and on the PSD of the noise sources Φ_{n_1} and Φ_{n_2}.

$$\Phi_{\delta x}(\omega) = |H_1(j\omega)|^2 \Phi_{n_1}(\omega) + |H_2(j\omega)|^2 \Phi_{n_2}(\omega) \tag{1.6}$$

If the two sensors have identical noise characteristics, $\Phi_{n_1}(\omega) = \Phi_{n_2}(\omega)$, a simple averaging ($H_1(s) = H_2(s) = 0.5$) is what would minimize the super sensor noise. This is the simplest form of sensor fusion with complementary filters.

However, the two sensors have usually high noise levels over distinct frequency regions. In such case, to lower the noise of the super sensor, the norm $|H_1(j\omega)|$ has to be small when $\Phi_{n_1}(\omega)$ is larger than $\Phi_{n_2}(\omega)$ and the norm $|H_2(j\omega)|$ has to be small when $\Phi_{n_2}(\omega)$ is larger than $\Phi_{n_1}(\omega)$. Hence, by properly shaping the norm of the complementary filters, it is possible to reduce the noise of the super sensor.

1.1.4 Sensor Fusion Robustness

In practical systems the sensor normalization is not perfect and condition (1.3) is not verified.

In order to study such imperfection, a multiplicative input uncertainty is added to the sensor dynamics (Fig. 1.5a). The nominal model is the estimated model used for the normalization $\hat{G}_i(s)$, $\Delta_i(s)$ is any stable transfer function satisfying $|\Delta_i(j\omega)| \leq 1$, $\forall \omega$, and $w_i(s)$ is a weighting transfer function representing the magnitude of the uncertainty.

The weight $w_i(s)$ is chosen such that the real sensor dynamics $G_i(j\omega)$ is contained in the uncertain region represented by a circle in the complex plane, centered on 1 and with a radius equal to $|w_i(j\omega)|$.

As the nominal sensor dynamics is taken as the normalized filter, the normalized sensor can be further simplified as shown in Fig. 1.5b.

(a) Sensor with multiplicative input uncertainty

(b) Simplified sensor model
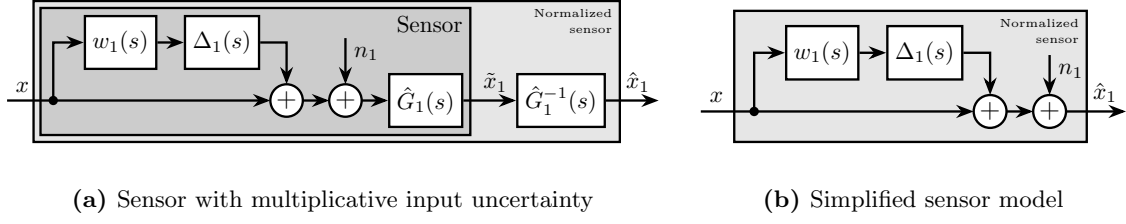
Figure 1.5: Sensor models with dynamical uncertainty

The sensor fusion architecture with the sensor models including dynamical uncertainty is shown in Fig. 1.6.
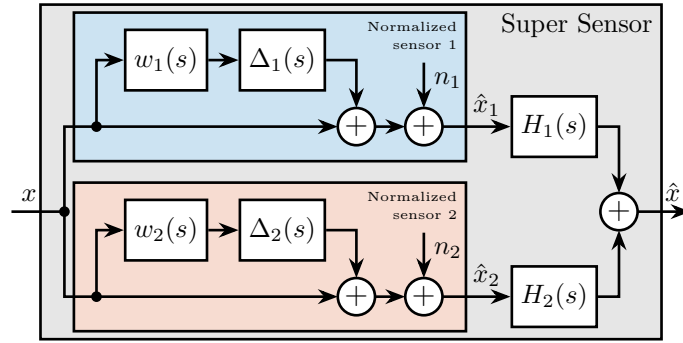

Figure 1.6: Sensor fusion architecture with sensor dynamics uncertainty

The super sensor dynamics (1.7) is no longer equal to 1 and now depends on the sensor dynamical uncertainty weights $w_i(s)$ as well as on the complementary filters $H_i(s)$.

$$\frac{\hat{x}}{x} = 1 + w_1(s)H_1(s)\Delta_1(s) + w_2(s)H_2(s)\Delta_2(s) \tag{1.7}$$

The dynamical uncertainty of the super sensor can be graphically represented in the complex plane by a circle centered on 1 with a radius equal to $|w_1(j\omega)H_1(j\omega)| + |w_2(j\omega)H_2(j\omega)|$ (Fig. 1.7).
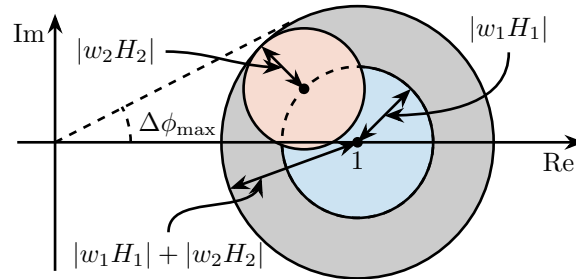
Figure 1.7: Uncertainty region of the super sensor dynamics in the complex plane (grey circle). The contribution of both sensors 1 and 2 to the total uncertainty are represented respectively by a blue circle and a red circle. The frequency dependency ω is here omitted.

10

The super sensor dynamical uncertainty, and hence the robustness of the fusion, clearly depends on the complementary filters' norm. For instance, the phase $\Delta\phi(\omega)$ added by the super sensor dynamics at frequency ω is bounded by $\Delta\phi_{\max}(\omega)$ which can be found by drawing a tangent from the origin to the uncertainty circle of the super sensor (Fig. 1.7) and that is mathematically described by (1.8).

$$\Delta\phi_{\max}(\omega) = \arcsin\left(|w_1(j\omega)H_1(j\omega)| + |w_2(j\omega)H_2(j\omega)|\right) \tag{1.8}$$

As it is generally desired to limit the maximum phase added by the super sensor, $H_1(s)$ and $H_2(s)$ should be designed such that $\Delta\phi$ is bounded to acceptable values. Typically, the norm of the complementary filter $|H_i(j\omega)|$ should be made small when $|w_i(j\omega)|$ is large, i.e., at frequencies where the sensor dynamics is uncertain.

1.2 Complementary Filters Shaping

As shown in Section 1.1, the noise and robustness of the super sensor are a function of the complementary filters' norm. Therefore, a synthesis method of complementary filters that allows to shape their norm would be of great use. In this section, such synthesis is proposed by writing the synthesis objective as a standard $\mathcal{H}_\infty$ optimization problem. As weighting functions are used to represent the wanted complementary filters' shape during the synthesis, their proper design is discussed. Finally, the synthesis method is validated on an simple example.

1.2.1 Synthesis Objective

The synthesis objective is to shape the norm of two filters $H_1(s)$ and $H_2(s)$ while ensuring their complementary property (1.1). This is equivalent as to finding proper and stable transfer functions $H_1(s)$ and $H_2(s)$ such that conditions (1.9a), (1.9b) and (1.9c) are satisfied.

$$H_1(s) + H_2(s) = 1 \tag{1.9a}$$

$$|H_1(j\omega)| \leq \frac{1}{|W_1(j\omega)|} \quad \forall\omega \tag{1.9b}$$

$$|H_2(j\omega)| \leq \frac{1}{|W_2(j\omega)|} \quad \forall\omega \tag{1.9c}$$

$W_1(s)$ and $W_2(s)$ are two weighting transfer functions that are carefully chosen to specify the maximum wanted norm of the complementary filters during the synthesis.

1.2.2 Shaping of Complementary Filters using $\mathcal{H}_\infty$ synthesis

In this section, it is shown that the synthesis objective can be easily expressed as a standard $\mathcal{H}_\infty$ optimization problem and therefore solved using convenient tools readily available.

Consider the generalized plant $P(s)$ shown in Fig. 1.8a and mathematically described by (1.10).

11

$$\begin{bmatrix} z_1 \\ z_2 \\ v \end{bmatrix} = P(s) \begin{bmatrix} w \\ u \end{bmatrix}; \quad P(s) = \begin{bmatrix} W_1(s) & -W_1(s) \\ 0 & W_2(s) \\ 1 & 0 \end{bmatrix} \tag{1.10}$$

(a) Generalized plant

(b) Generalized plant with the synthesized filter
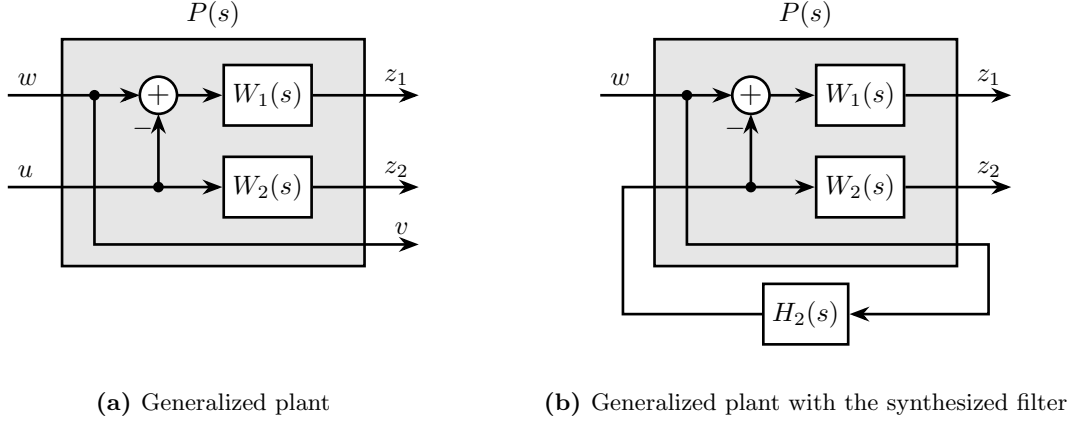
Figure 1.8: Architecture for the $\mathcal{H}_\infty$ synthesis of complementary filters

Applying the standard $\mathcal{H}_\infty$ synthesis to the generalized plant $P(s)$ is then equivalent as finding a stable filter $H_2(s)$ which based on v, generates a signal u such that the $\mathcal{H}_\infty$ norm of the system in Fig. 1.8b from w to $[z_1, \ z_2]$ is less than one (1.11).

$$\left\| \begin{matrix} (1 - H_2(s))\, W_1(s) \\ H_2(s) W_2(s) \end{matrix} \right\|_\infty \leq 1 \tag{1.11}$$

By then defining $H_1(s)$ to be the complementary of $H_2(s)$ (1.12), the $\mathcal{H}_\infty$ synthesis objective becomes equivalent to (1.13) which ensures that (1.9b) and (1.9c) are satisfied.

$$H_1(s)1 - H_2(s) \tag{1.12}$$

$$\left\| \begin{matrix} H_1(s) W_1(s) \\ H_2(s) W_2(s) \end{matrix} \right\|_\infty \leq 1 \tag{1.13}$$

Therefore, applying the $\mathcal{H}_\infty$ synthesis to the standard plant $P(s)$ (1.10) will generate two filters $H_2(s)$ and $H_1(s)1 - H_2(s)$ that are complementary (1.9) and such that there norms are bellow specified bounds (1.9b), (1.9c).

Note that there is only an implication between the $\mathcal{H}_\infty$ norm condition (1.13) and the initial synthesis objectives (1.9b) and (1.9c) and not an equivalence. Hence, the optimization may be a little bit conservative with respect to the set of filters on which it is performed, see [29, Chap. 2.8.3]. In practice, this is however not an found to be an issue.

1.2.3 Weighting Functions Design

Weighting functions are used during the synthesis to specify the maximum allowed complementary filters' norm. The proper design of these weighting functions is of primary importance for the success of the presented $\mathcal{H}_\infty$ synthesis of complementary filters.

First, only proper and stable transfer functions should be used. Second, the order of the weighting functions should stay reasonably small in order to reduce the computational costs associated with the solving of the optimization problem and for the physical implementation of the filters (the synthesized filters' order being equal to the sum of the weighting functions' order). Third, one should not forget the fundamental limitations imposed by the complementary property (1.1). This implies for instance that $|H_1(j\omega)|$ and $|H_2(j\omega)|$ cannot be made small at the same frequency.

When designing complementary filters, it is usually desired to specify their slopes, their "blending" frequency and their maximum gains at low and high frequency. To easily express these specifications, formula (1.14) is proposed to help with the design of weighting functions.

$$
W(s) = \left(\frac{\frac{1}{\omega_c} \sqrt{\frac{1-\left(\frac{G_0}{G_c}\right)^{\frac{2}{n}}}{1-\left(\frac{G_c}{G_\infty}\right)^{\frac{2}{n}}}} s + \left(\frac{G_0}{G_c}\right)^{\frac{1}{n}}}{\left(\frac{1}{G_\infty}\right)^{\frac{1}{n}} \frac{1}{\omega_c} \sqrt{\frac{1-\left(\frac{G_0}{G_c}\right)^{\frac{2}{n}}}{1-\left(\frac{G_c}{G_\infty}\right)^{\frac{2}{n}}}} s + \left(\frac{1}{G_c}\right)^{\frac{1}{n}}} \right)^n
\tag{1.14}
$$

The parameters in formula (1.14) are:

- $G_0 = \lim_{\omega \to 0} |W(j\omega)|$: the low frequency gain

- $G_\infty = \lim_{\omega \to \infty} |W(j\omega)|$: the high frequency gain

- $G_c = |W(j\omega_c)|$: the gain at a specific frequency ω_c in rad/s.

- n: the slope between high and low frequency. It also corresponds to the order of the weighting function.

The parameters G_0, G_c and G_∞ should either satisfy (1.15a) or (1.15b).

$$
G_0 < 1 < G_\infty \text{ and } G_0 < G_c < G_\infty
\tag{1.15a}
$$
$$
G_\infty < 1 < G_0 \text{ and } G_\infty < G_c < G_0
\tag{1.15b}
$$

The typical magnitude of a weighting function generated using (1.14) is shown in Fig. 1.9.

1.2.4 Validation of the proposed synthesis method

The proposed methodology for the design of complementary filters is now applied on a simple example. Let's suppose two complementary filters $H_1(s)$ and $H_2(s)$ have to be designed such that:
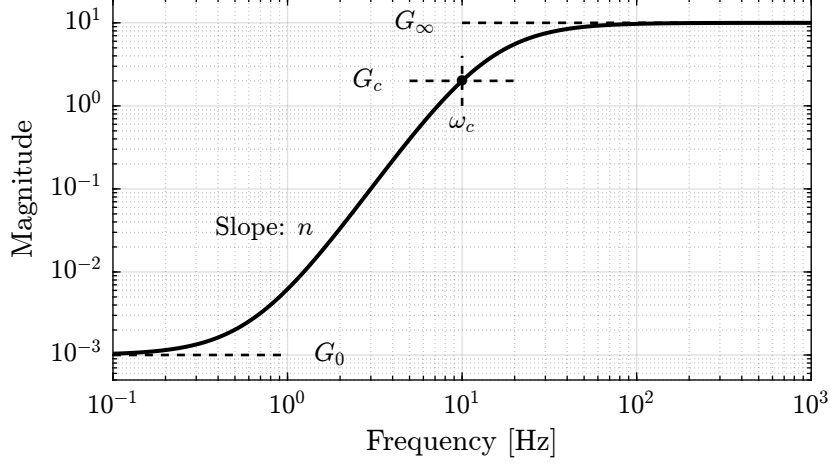
Figure 1.9: Magnitude of a weighting function generated using formula (1.14), $G_0 = 1e^{-3}$, $G_\infty = 10$, $\omega_c = 10Hz$, $G_c = 2$, $n = 3$.

- the blending frequency is around $10Hz$.

- the slope of $|H_1(j\omega)|$ is $+2$ below $10Hz$. Its low frequency gain is 10^{-3}.

- the slope of $|H_2(j\omega)|$ is -3 above $10Hz$. Its high frequency gain is 10^{-3}.

The first step is to translate the above requirements by properly designing the weighting functions. The proposed formula (1.14) is here used for such purpose. Parameters used are summarized in Table 1.1. The inverse magnitudes of the designed weighting functions, which are representing the maximum allowed norms of the complementary filters, are shown by the dashed lines in Fig. 1.10.

Parameter	$W_1(s)$	$W_2(s)$
G_0	0.1	1000
G_∞	1000	0.1
ω_c	$2\pi \cdot 10$	$2\pi \cdot 10$
G_c	0.45	0.45
n	2	3
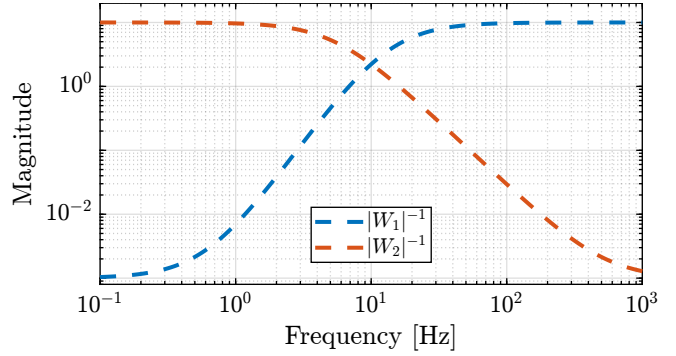
Table 1.1: Parameters for $W_1(s)$ and $W_2(s)$ **Figure 1.10:** Inverse magnitude of the weights

The standard $\mathcal{H}_\infty$ synthesis is then applied to the generalized plant of Fig. 1.8a. The filter $H_2(s)$ that minimizes the $\mathcal{H}_\infty$ norm between w and $[z_1, \ z_2]^T$ is obtained. The $\mathcal{H}_\infty$ norm is here found to be close to one (1.16) which indicates that the synthesis is successful: the complementary filters norms are below the maximum specified upper bounds. This is confirmed by the bode plots of the obtained complementary filters in Fig. 1.11.

$$\left\| \begin{matrix} (1 - H_2(s))\, W_1(s) \\ H_2(s) W_2(s) \end{matrix} \right\|_\infty \approx 1 \tag{1.16}$$

14

The transfer functions in the Laplace domain of the complementary filters are given in (1.17). As expected, the obtained filters are of order 5, that is the sum of the weighting functions' order.

$$H_2(s) = \frac{(s + 6.6e^4)(s + 160)(s + 4)^3}{(s + 6.6e^4)(s^2 + 106s + 3e^3)(s^2 + 72s + 3580)} \tag{1.17a}$$

$$H_1(s)H_2(s) - 1 = \frac{10^{-8}(s + 6.6e^9)(s + 3450)^2(s^2 + 49s + 895)}{(s + 6.6e^4)(s^2 + 106s + 3e^3)(s^2 + 72s + 3580)} \tag{1.17b}$$
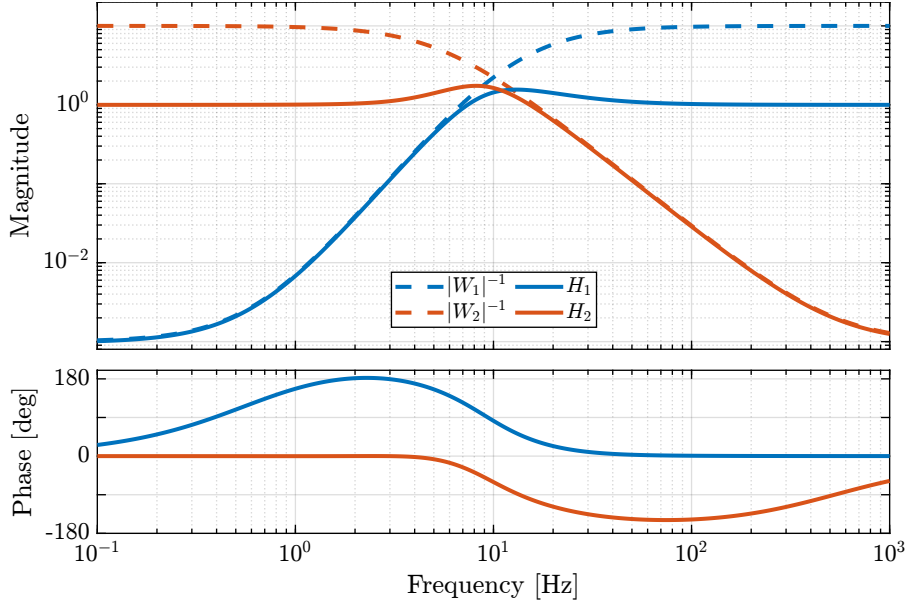

Figure 1.11: Bode plot of the obtained complementary filters

This simple example illustrates the fact that the proposed methodology for complementary filters shaping is easy to use and effective. A more complex real life example is taken up in the next section.

1.3 "Closed-Loop" complementary filters

An alternative way to implement complementary filters is by using a fundamental property of the classical feedback architecture shown in Fig. 1.12. This idea is discussed in [9], [14], [30].
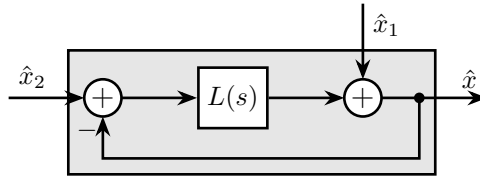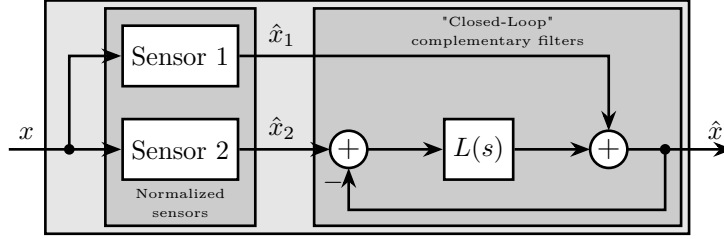

Figure 1.12: "Closed-Loop" complementary filters.

Consider the feedback architecture of Fig. 1.12, with two inputs $\hat{x}_1$ and $\hat{x}_2$, and one output $\hat{x}$. The output $\hat{x}$ is linked to the inputs by (1.18).

$$\hat{x} = \underbrace{\frac{1}{1 + L(s)}}_{S(s)} \hat{x}_1 + \underbrace{\frac{L(s)}{1 + L(s)}}_{T(s)} \hat{x}_2 \tag{1.18}$$

As for any classical feedback architecture, we have that the sum of the sensitivity transfer function $S(s)$ and complementary sensitivity transfer function $T(s)$ is equal to one (1.19).

$$S(s) + T(s) = 1 \tag{1.19}$$

Therefore, provided that the the closed-loop system in Fig. 1.12 is stable, it can be used as a set of two complementary filters. Two sensors can then be merged as shown in Fig. 1.13.

Figure 1.13: Classical feedback architecture used for sensor fusion.

One of the main advantage of implementing and designing complementary filters using the feedback architecture of Fig. 1.12 is that all the tools of the linear control theory can be applied for the design of the filters. If one want to shape both $\frac{\hat{x}}{\hat{x}_1}(s) = S(s)$ and $\frac{\hat{x}}{\hat{x}_2}(s) = T(s)$, the $\mathcal{H}_\infty$ mixed-sensitivity synthesis can be easily applied.

To do so, weighting functions $W_1(s)$ and $W_2(s)$ are added to respectively shape $S(s)$ and $T(s)$ (Fig. 1.14a). Then the system is rearranged to form the generalized plant $P_L(s)$ shown in Fig. 1.14b. The $\mathcal{H}_\infty$ mixed-sensitivity synthesis can finally be performed by applying the standard $\mathcal{H}_\infty$ synthesis to the generalized plant $P_L(s)$ which is described by (1.20).

$$\begin{bmatrix} z \\ v \end{bmatrix} = P_L(s) \begin{bmatrix} w_1 \\ w_2 \\ u \end{bmatrix}; \quad P_L(s) = \begin{bmatrix} W_1(s) & 0 & 1 \\ -W_1(s) & W_2(s) & -1 \end{bmatrix} \tag{1.20}$$

The output of the synthesis is a filter $L(s)$ such that the "closed-loop" $\mathcal{H}_\infty$ norm from $[w_1,\ w_2]$ to z of the system in Fig. 1.12 is less than one (1.21).

$$\left\| \begin{matrix} \frac{z}{w_1} \\ \frac{z}{w_2} \end{matrix} \right\|_\infty = \left\| \begin{matrix} \frac{1}{1+L(s)} W_1(s) \\ \frac{L(s)}{1+L(s)} W_2(s) \end{matrix} \right\|_\infty \leq 1 \tag{1.21}$$

If the synthesis is successful, the transfer functions from $\hat{x}_1$ to $\hat{x}$ and from $\hat{x}_2$ to $\hat{x}$ have their magnitude bounded by the inverse magnitude of the corresponding weighting functions. The sensor fusion can then be implemented using the feedback architecture in Fig. 1.13 or more classically as shown in Fig. 1.2 by defining the two complementary filters using (1.22). The two architectures are equivalent regarding their inputs/outputs relationships.

$$H_1(s) = \frac{1}{1 + L(s)}; \quad H_2(s) = \frac{L(s)}{1 + L(s)} \tag{1.22}$$

(a) Feedback architecture with included weights   **(b)** Generalized plant
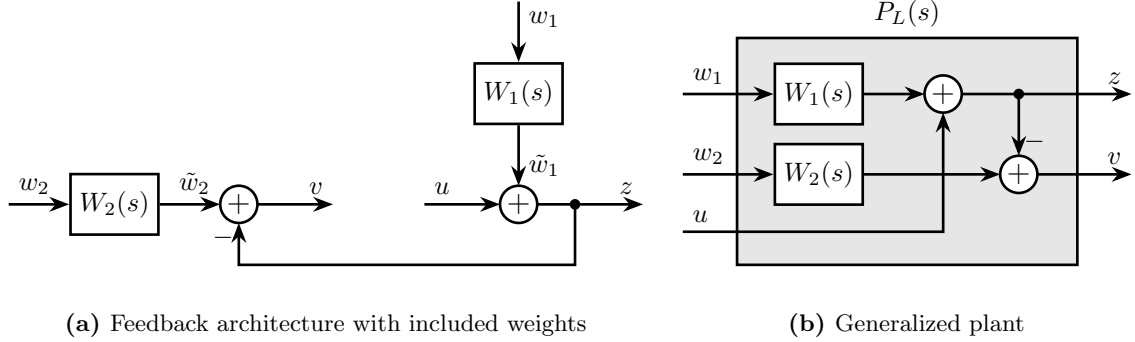
Figure 1.14: $\mathcal{H}_\infty$ mixed-sensitivity synthesis

As an example, two "closed-loop" complementary filters are designed using the $\mathcal{H}_\infty$ mixed-sensitivity synthesis. The weighting functions are designed using formula (1.14) with parameters shown in Table 1.1. After synthesis, a filter $L(s)$ is obtained whose magnitude is shown in Fig. 1.15 by the black dashed line. The "closed-loop" complementary filters are compared with the inverse magnitude of the weighting functions in Fig. 1.15 confirming that the synthesis is successful. The obtained "closed-loop" complementary filters are indeed equal to the ones obtained in Section 1.2.4.
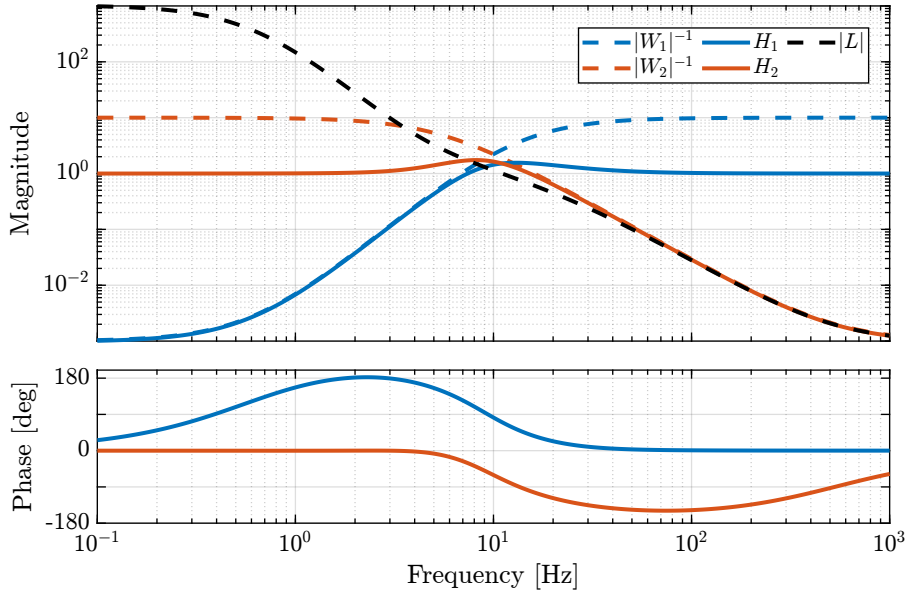

Figure 1.15: Bode plot of the obtained complementary filters after $\mathcal{H}_\infty$ mixed-sensitivity synthesis

1.4 Synthesis of a set of three complementary filters

Some applications may require to merge more than two sensors [23], [26]. For instance at the LIGO, three sensors (an LVDT, a seismometer and a geophone) are merged to form a super sensor [27].

When merging $n > 2$ sensors using complementary filters, two architectures can be used as shown in Fig. 1.16. The fusion can either be done in a "sequential" way where $n-1$ sets of two complementary filters are used (Fig. 1.16a), or in a "parallel" way where one set of n complementary filters is used (Fig. 1.16b).

In the first case, typical sensor fusion synthesis techniques can be used. However, when a parallel architecture is used, a new synthesis method for a set of more than two complementary filters is required as only simple analytical formulas have been proposed in the literature [23], [26]. A generalization of the proposed synthesis method of complementary filters is presented in this section.

(a) Sequential fusion **(b)** Parallel fusion
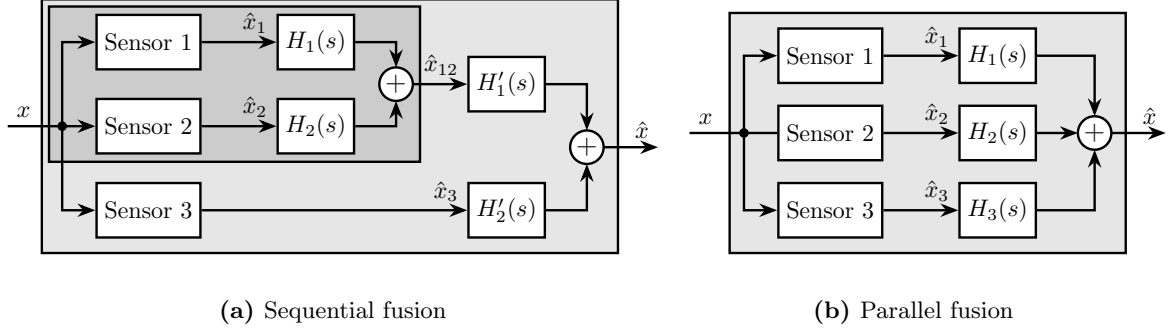
Figure 1.16: Possible sensor fusion architecture when more than two sensors are to be merged

The synthesis objective is to compute a set of n stable transfer functions $[H_1(s), H_2(s), \ldots, H_n(s)]$ such that conditions (1.23a) and (1.23b) are satisfied.

$$\sum_{i=1}^{n} H_i(s) = 1 \tag{1.23a}$$

$$|H_i(j\omega)| < \frac{1}{|W_i(j\omega)|}, \quad \forall \omega, \ i = 1 \ldots n \tag{1.23b}$$

$[W_1(s), W_2(s), \ldots, W_n(s)]$ are weighting transfer functions that are chosen to specify the maximum complementary filters' norm during the synthesis.

Such synthesis objective is closely related to the one described in Section 1.2.1, and indeed the proposed synthesis method is a generalization of the one presented in Section 1.2.2.

A set of n complementary filters can be shaped by applying the standard $\mathcal{H}_\infty$ synthesis to the generalized plant $P_n(s)$ described by (1.24).

$$\begin{bmatrix} z_1 \\ \vdots \\ z_n \\ v \end{bmatrix} = P_n(s) \begin{bmatrix} w \\ u_1 \\ \vdots \\ u_{n-1} \end{bmatrix}; \quad P_n(s) = \begin{bmatrix} W_1 & -W_1 & \ldots & \ldots & -W_1 \\ 0 & W_2 & 0 & \ldots & 0 \\ \vdots & \ddots & \ddots & \ddots & \vdots \\ \vdots & & \ddots & \ddots & 0 \\ 0 & \ldots & \ldots & 0 & W_n \\ 1 & 0 & \ldots & \ldots & 0 \end{bmatrix} \tag{1.24}$$

If the synthesis if successful, a set of $n-1$ filters $[H_2(s), H_3(s), \ldots, H_n(s)]$ are obtained such that (1.25) is verified.

$$\left\| \begin{matrix} \left(1 - [H_2(s) + H_3(s) + \cdots + H_n(s)]\right) W_1(s) \\ H_2(s)W_2(s) \\ \vdots \\ H_n(s)W_n(s) \end{matrix} \right\|_\infty \leq 1 \tag{1.25}$$
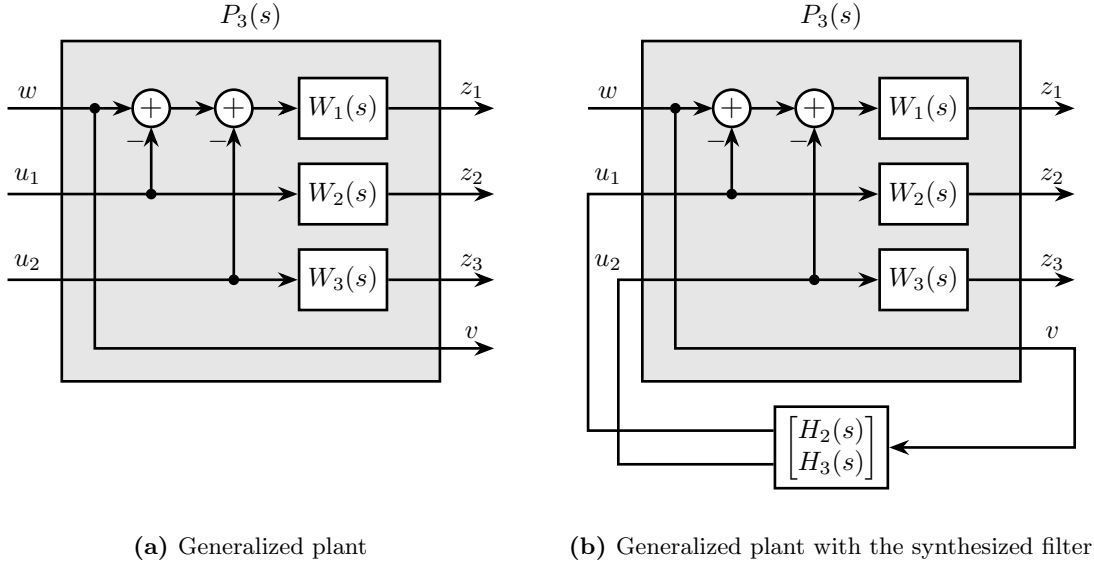
$H_1(s)$ is then defined using (1.26) which is ensuring the complementary property for the set of n filters (1.23a). Condition (1.23b) is satisfied thanks to (1.25).

$$H_1(s)1 - \left[H_2(s) + H_3(s) + \cdots + H_n(s) \right] \tag{1.26}$$

An example is given to validate the proposed method for the synthesis of a set of three complementary filters. The sensors to be merged are a displacement sensor from DC up to $1Hz$, a geophone from 1 to $10Hz$ and an accelerometer above $10Hz$. Three weighting functions are designed using formula (1.14) and their inverse magnitude are shown in Fig. 1.18 (dashed curves).

Consider the generalized plant $P_3(s)$ shown in Fig. 1.17a which is also described by (1.27).

$$\begin{bmatrix} z_1 \\ z_2 \\ z_3 \\ v \end{bmatrix} = P_3(s) \begin{bmatrix} w \\ u_1 \\ u_2 \end{bmatrix} ; \quad P_3(s) = \begin{bmatrix} W_1(s) & -W_1(s) & -W_1(s) \\ 0 & W_2(s) & 0 \\ 0 & 0 & W_3(s) \\ 1 & 0 & 0 \end{bmatrix} \tag{1.27}$$

**(a)** Generalized plant   **(b)** Generalized plant with the synthesized filter

Figure 1.17: Architecture for the $\mathcal{H}_\infty$ synthesis of three complementary filters

The standard $\mathcal{H}_\infty$ synthesis is performed on the generalized plant $P_3(s)$. Two filters $H_2(s)$ and $H_3(s)$ are obtained such that the $\mathcal{H}_\infty$ norm of the closed-loop transfer from w to $[z_1, z_2, z_3]$ of the system

in Fig. 1.17b is less than one. Filter $H_1(s)$ is defined using (1.28) thus ensuring the complementary property of the obtained set of filters.

$$H_1(s)1 - \left[H_2(s) + H_3(s) \right] \tag{1.28}$$

Figure 1.18 displays the three synthesized complementary filters (solid lines) which confirms that the synthesis is successful.
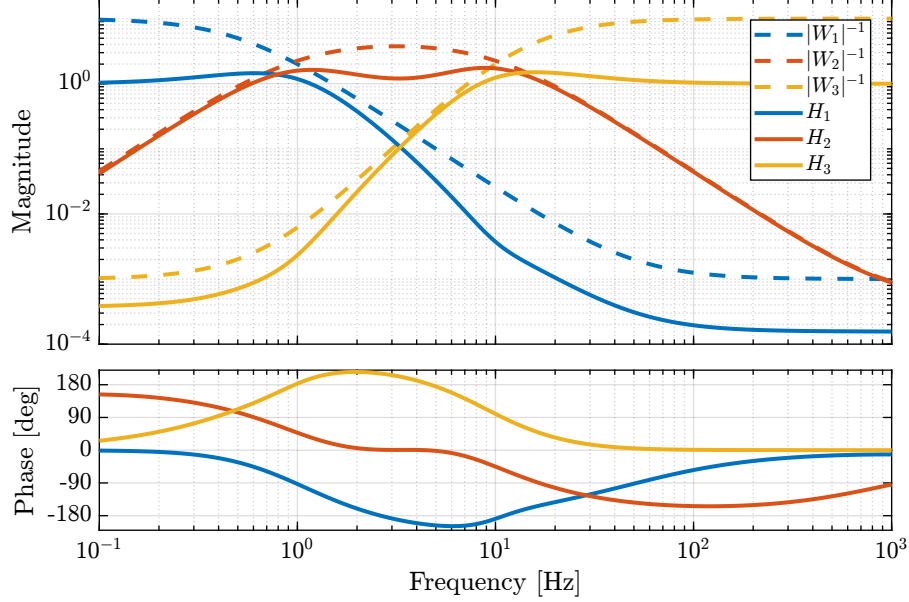
Figure 1.18: Bode plot of the inverse weighting functions and of the three complementary filters obtained using the $\mathcal{H}_\infty$ synthesis

Conclusion

A new method for designing complementary filters using the $\mathcal{H}_\infty$ synthesis has been proposed. It allows to shape the magnitude of the filters by the use of weighting functions during the synthesis. This is very valuable in practice as the characteristics of the super sensor are linked to the complementary filters' magnitude. Therefore typical sensor fusion objectives can be translated into requirements on the magnitudes of the filters. Several examples were used to emphasize the simplicity and the effectiveness of the proposed method.

However, the shaping of the complementary filters' magnitude does not allow to directly optimize the super sensor noise and dynamical characteristics. Future work will aim at developing a complementary filter synthesis method that minimizes the super sensor noise while ensuring the robustness of the fusion.

2 Decoupling Strategies

When dealing with MIMO systems, a typical strategy is to:

- first decouple the plant dynamics

- apply SISO control for the decoupled plant

Assumptions:

- parallel manipulators

Review of decoupling strategies for Stewart platforms:

- Decoupling Strategies

    What example should be taken? **3dof system**? stewart platform? Maybe simpler.

2.1 Interaction Analysis

2.2 Decentralized Control (actuator frame)

2.3 Center of Stiffness and center of Mass

- Example

- Show

2.4 Modal Decoupling

2.5 Data Based Decoupling

- Static decoupling

- SVD

Conclusion

Table that compares all the strategies.

3 Closed-Loop Shaping using Complementary Filters

Performance of a feedback control is dictated by closed-loop transfer functions. For instance sensitivity, transmissibility, etc... Gang of Four.

There are several ways to design a controller to obtain a given performance.

Decoupled Open-Loop Shaping:

- As shown in previous section, once the plant is decoupled: open loop shaping

- Explain procedure when applying open-loop shaping

- Lead, Lag, Notches, Check Stability, c2d, etc...

- But this is open-loop shaping, and it does not directly work on the closed loop transfer functions

Other strategy: Model Based Design:

- Multivariable Control

- Talk about Caio's thesis?

- Review of model based design (LQG, H-Infinity) applied to Stewart platform

- Difficulty to specify robustness to change of payload mass

In this section, an alternative is proposed in which complementary filters are used for closed-loop shaping. It is presented for a SISO system, but can be generalized to MIMO if decoupling is sufficient. It will be experimentally demonstrated with the NASS.

Conclusion

Conclusion

Bibliography

[1] M. A. Beijen, D. Tjepkema, and J. van Dijk, "Two-sensor control in active vibration isolation using hard mounts," *Control Engineering Practice*, vol. 26, pp. 82–90, 2014 (cit. on p. 4).

[2] Y. K. Yong and A. J. Fleming, "High-speed vertical positioning stage with integrated dual-sensor arrangement," *Sensors and Actuators A: Physical*, vol. 248, pp. 184–192, 2016 (cit. on pp. 4, 6).

[3] J. Bendat, "Optimum filters for independent measurements of two related perturbed messages," *IRE Transactions on Circuit Theory*, 1957 (cit. on p. 6).

[4] F. Shaw and K. Srinivasan, "Bandwidth enhancement of position measurements using measured acceleration," *Mechanical Systems and Signal Processing*, vol. 4, no. 1, pp. 23–38, 1990 (cit. on p. 6).

[5] M. Zimmermann and W. Sulzer, "High bandwidth orientation measurement and control based on complementary filtering," *Robot Control 1991*, Robot Control 1991, pp. 525–530, 1992 (cit. on p. 6).

[6] H. G. Min and E. T. Jeung, "Complementary filter design for angle estimation using mems accelerometer and gyroscope," *Department of Control and Instrumentation, Changwon National University, Changwon, Korea*, pp. 641–773, 2015 (cit. on p. 6).

[7] W. Hua, "Low frequency vibration isolation and alignment system for advanced ligo," Ph.D. dissertation, stanford university, 2005 (cit. on p. 6).

[8] W. Hua, D. B. Debra, C. T. Hardham, B. T. Lantz, and J. A. Giaime, "Polyphase fir complementary filters for control systems," in *Proceedings of ASPE Spring Topical Meeting on Control of Precision Systems*, 2004, pp. 109–114 (cit. on p. 6).

[9] A. R. Plummer, "Optimal complementary filters and their application in motion measurement," *Proceedings of the Institution of Mechanical Engineers, Part I: Journal of Systems and Control Engineering*, vol. 220, no. 6, pp. 489–507, 2006 (cit. on pp. 6, 15).

[10] P. Y. C. H. Robert Grover Brown, *Introduction to Random Signals and Applied Kalman Filtering with Matlab Exercises*, 4th ed. Wiley, 2012 (cit. on p. 6).

[11] C. Collette and F. Matichard, "Sensor fusion methods for high performance active vibration isolation systems," *Journal of Sound and Vibration*, vol. 342, pp. 1–21, 2015 (cit. on p. 6).

[12] A.-J. Baerveldt and R. Klang, "A low-cost and low-weight attitude estimation system for an autonomous helicopter," in *Proceedings of IEEE International Conference on Intelligent Engineering Systems*, 1997 (cit. on p. 6).

[13] P. Corke, "An inertial and visual sensing system for a small autonomous helicopter," *Journal of Robotic Systems*, vol. 21, no. 2, pp. 43–51, 2004 (cit. on p. 6).

[14] A. Jensen, C. Coopmans, and Y. Chen, "Basics and guidelines of complementary filters for small uas navigation," in *2013 International Conference on Unmanned Aircraft Systems (ICUAS)*, May 2013 (cit. on pp. 6, 15).

[15] A. Pascoal, I. Kaminer, and P. Oliveira, "Navigation system design using time-varying complementary filters," in *Guidance, Navigation, and Control Conference and Exhibit*, 1999 (cit. on p. 6).

[16] P. Batista, C. Silvestre, and P. Oliveira, "Optimal position and velocity navigation filters for autonomous vehicles," *Automatica*, vol. 46, no. 4, pp. 767–774, 2010 (cit. on p. 6).

[17] D. Tjepkema, J. van Dijk, and H. Soemers, "Sensor fusion for active vibration isolation in precision equipment," *Journal of Sound and Vibration*, vol. 331, no. 4, pp. 735–749, 2012 (cit. on p. 6).

[18] J. van Heijningen, "Low-frequency performance improvement of seismic attenuation systems and vibration sensors for next generation gravitational wave detectors," Ph.D. dissertation, Vrije Universiteit, 2018 (cit. on p. 6).

[19] T. Lucia, "Low frequency optimization and performance of advanced virgo seismic isolation system," Ph.D. dissertation, University of Siena, 2018 (cit. on p. 6).

[20] W. Anderson and E. Fritze, "Instrument approach system steering computer," *Proceedings of the IRE*, vol. 41, no. 2, pp. 219–228, 1953 (cit. on p. 6).

[21] R. G. Brown, "Integrated navigation systems and kalman filtering: A perspective," *Navigation*, vol. 19, no. 4, pp. 355–362, 1972 (cit. on p. 6).

[22] W. T. Higgins, "A comparison of complementary and kalman filtering," *IEEE Transactions on Aerospace and Electronic Systems*, no. 3, pp. 321–325, 1975 (cit. on p. 6).

[23] F. P. N. da Fonseca Cardoso, J. M. F. Calado, C. B. Cardeira, P. J. C. R. Oliveira, et al., "Complementary filter design with three frequency bands: Robot attitude estimation," in *2015 IEEE International Conference on Autonomous Robot Systems and Competitions*, IEEE, 2015, pp. 168–173 (cit. on pp. 6, 17, 18).

[24] S. I. Moore, A. J. Fleming, and Y. K. Yong, "Capacitive instrumentation and sensor fusion for high-bandwidth nanopositioning," *IEEE Sensors Letters*, vol. 3, no. 8, pp. 1–3, 2019 (cit. on p. 6).

[25] T.-J. Yeh, C.-Y. Su, and W.-J. Wang, "Modelling and control of a hydraulically actuated two-degree-of-freedom inertial platform," *Proceedings of the Institution of Mechanical Engineers, Part I: Journal of Systems and Control Engineering*, vol. 219, no. 6, pp. 405–417, 2005 (cit. on p. 6).

[26] D. Stoten, "Fusion of kinetic data using composite filters," *Proceedings of the Institution of Mechanical Engineers, Part I: Journal of Systems and Control Engineering*, vol. 215, no. 5, pp. 483–497, 2001 (cit. on pp. 6, 17, 18).

[27] F. Matichard, B. Lantz, R. Mittleman, et al., "Seismic isolation of advanced ligo: Review of strategy, instrumentation and performance," *Classical and Quantum Gravity*, vol. 32, no. 18, p. 185 003, 2015 (cit. on pp. 6, 17).

[28] T. Dehaeze, M. Vermat, and C. Collette, "Complementary filters shaping using $\mathcal{H}_\infty$ synthesis," in *7th International Conference on Control, Mechatronics and Automation (ICCMA)*, 2019, pp. 459–464 (cit. on pp. 6, 7).

[29] S. Skogestad and I. Postlethwaite, *Multivariable Feedback Control: Analysis and Design - Second Edition*. John Wiley, 2007 (cit. on p. 12).

[30] R. Mahony, T. Hamel, and J.-M. Pflimlin, "Complementary filter design on the special orthogonal group so(3)," in *Proceedings of the 44th IEEE Conference on Decision and Control*, 2005 (cit. on p. 15).